Emulsion-Templated Gold Beads Using Gold Nanoparticles as Building Blocks**

By *Haifei Zhang*, *Irshad Hussain*, *Mathias Brust*, and *Andrew I. Cooper**

In this paper, we describe a new method for preparing highly porous gold beads by using emulsion-templated polymers[1,2] as scaffolds. Porous noble metals have potential applications as catalysts,[3] as biosensors,[4,5] and as porous electrodes. For example, porous gold has been used for the detection of biomolecules using ellipsometry[4] or quartz crystal microbalance technology.[5]

There are a number of methods for generating porous gold structures. Nanoporous gold nanowires[6] and gold with a multimodal pore size distribution[7] have been prepared by selective etching of the silver phase from gold–silver alloys (also known as dealloying).[8] Macroporous gold materials (i.e., pore sizes > 50 nm) can be prepared by templating routes such as colloidal crystal templating.[9,10] Less highly ordered macroporous gold structures with 15 μm channels were prepared by templating the calcium carbonate skeletal plates of echinoids (sea urchins),[11] while macroporous silver, gold, and metal oxide sponges have been prepared from metal-salt-containing dextran pastes.[12] The latter represents a versatile method for producing porous metals in a "monolithic" (i.e., molded) format.

The preparation of porous particles of noble metals has received less attention. Two new approaches have been described very recently. The first involves the sonication of a silica-gold nanoparticle dispersion to form discrete silica-gold composite spheres (< 1 μm) with a range of morphologies.[13] The second involves templating commercially available crosslinked polystyrene microspheres to produce porous gold beads of around 9 μm diameter.[14] In this process, the polystyrene template was soaked in a concentrated gold sol (2 $g\,L^{-1}$), the excess sol removed by filtration, and the polymer phase removed by calcination. The beaded morphology was retained in the products, and the average pore size in the materials was found to be in the range 50–80 nm.

We report here a new method for the preparation of emulsion-templated gold in the form of uniform beads (size range 0.5–1 mm). Large porous beads are useful, for example, in applications such as catalysis due to ease of separation. In our process, emulsion-templated crosslinked polyacrylamide (PAM) beads were synthesized by "oil-in-water-in-oil" (O/W/O) sedimentation polymerization, as described previously.[1,15] These beads were then soaked in an aqueous gold sol (average gold particle diameter = 15 nm, concentration = 0.15 $g\,L^{-1}$) that had been prepared using sodium acrylate as the reducing agent and stabilizing ligand.[16] It was observed that the PAM beads turned an intense red color, while the gold sol (which was originally deep red in color) became mostly decolored (Figure 1a).

In order to test whether the adsorption of the gold particles onto the polymer was reversible, the beads were separated by filtration and submerged in fresh water. No color was observed in the solution after one day, even when the beads were fractured and the solution was sonicated. This suggests that the gold particles were strongly bound to the polymer surface. We are not aware of previous reports on the use of primary amides (as found in PAM) for the adsorption of gold nanoparticles, although it is well known that alkyl amines can adsorb at the surface of gold nanoparticles[17] and can be used to tether gold to surfaces such as zeolites.[18] When the gold–PAM composite beads were filtered and dried, the beads shrank dramatically. The color of the beads in the dry, shrunken state was much darker (tending towards black), but the original red color returned if the beads were swollen again with water. This indicates that the gold particles did not aggregate irreversibly, even when the beads shrank, since it is known that particle aggregation leads to a distinct color change (from red to blue/purple) for gold particles in this approximate size range.[16,19,20]

In order to prepare uniform, emulsion-templated gold beads, two problems had to be addressed. The first was to avoid the high degree of shrinkage during drying of the PAM–gold composite, since this largely destroys the emulsion-templated structure. This was solved by soaking the wet composite beads immediately after filtration in an excess of isopropanol for five hours, filtering, and then drying in air (c.f., preparation of aerogels[21]). The second challenge was to achieve sufficiently high gold loadings such that stable gold beads could be formed after calcining the polymer phase. Fortunately, the PAM matrix concentrates the gold nanoparticles on itself by adsorption; as such, a highly concentrated gold sol was not required to achieve gold loadings of more than 90 wt.-% (i.e., the sample mass almost doubled).

It was found that the distribution of the gold particles through the bead structure could be controlled by adjusting the ratio of gold to polymer and, to some extent, by changing the immersion time. Figure 1b shows a cross-section of a gold–polymer composite bead prepared under "nanoparticle starved" conditions. In this case, a gold-functionalized "shell"

[*] Dr. A. I. Cooper, Dr. H. Zhang, I. Hussain, Dr. M. Brust
Donnan and Robert Robinson Laboratories
Department of Chemistry, University of Liverpool
Crown Street, Liverpool L69 3BX (UK)
E-mail: aicooper@liv.ac.uk

I. Hussain
National Institute for Biotechnology and
Genetic Engineering (NIBGE)
P.O. Box 577, Jhang Road, Faisalabad (Pakistan)

[**] The authors acknowledge The Royal Society for a University Research Fellowship (to AIC) and the Engineering and Physical Sciences Research Council (EPSRC) for financial support (GR/N39999+GR/R15597). IH thanks NIBGE and the Ministry of Science and Technology, Government of Pakistan, for funding. MB thanks the EPSRC for an Advanced Research Fellowship. We thank Georgina Hardy for assistance with the calcination of the materials.

DOI: 10.1002/adma.200306153

ADVANCED MATERIALS

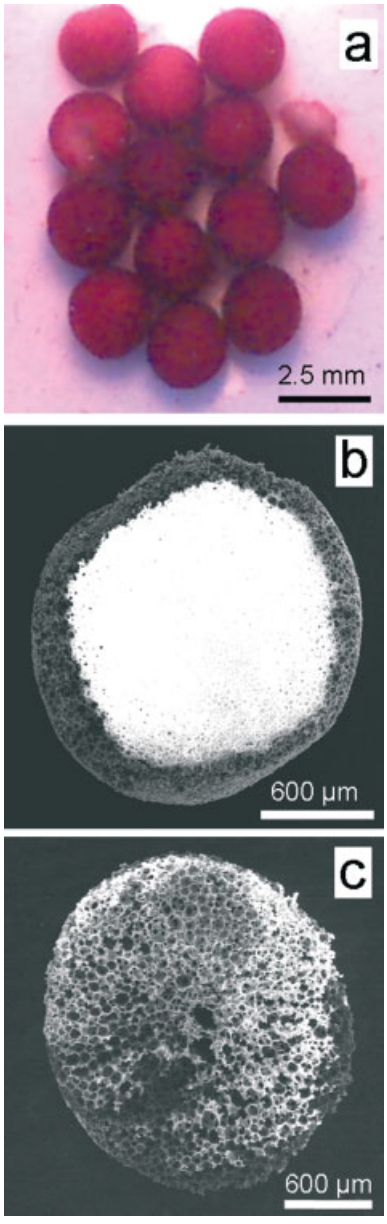

Figure 1. a) Optical micrograph of gold–polymer composite beads showing almost complete decolorization of the surrounding gold sol. b) Electron micrograph of a cross-sectioned gold–polymer composite bead with a non-uniform distribution of gold nanoparticles. The uncoated polymer appears bright due to "charging". c) Electron micrograph of a cross-sectioned gold–polymer composite bead with a more uniform distribution of metal nanoparticles. The composite retains the original emulsion-templated pore structure.

was formed around the periphery of the porous bead, which extended approximately 150 µm into the interior of the structure. The centre of the bead was devoid of gold nanoparticles, as evidenced by a lack of color (visible under an optical microscope) and a high degree of "charging" in the electron micrograph (Fig. 1b). It was also possible to generate materials with a uniform distribution of particles throughout the whole bead (Fig. 1c) by increasing the ratio of gold particles to polymer or by replenishing the supernatant liquid with particles as it became decolored during soaking.

Figure 2 shows optical micrographs of templated gold beads formed by calcination of uniformly gold-functionalized PAM beads at 520 °C in air. Microanalysis of the products indicated

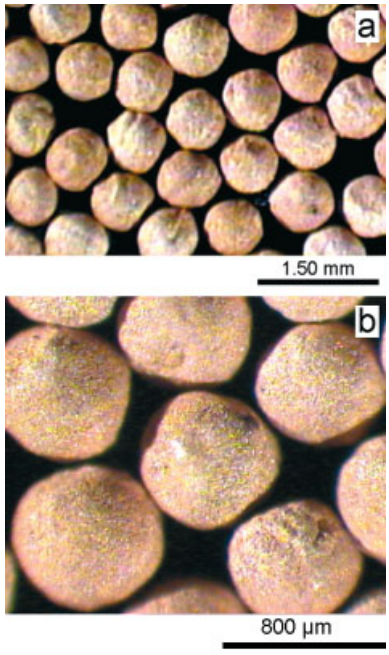

Figure 2. Optical micrographs of emulsion-templated gold beads after calcination of the polymer phase at 520 °C.

that the organic phase was mostly removed (C 0.41 %, H 0 %, N 0 %, Na 1.75 %, Au 94.85 %). The residual sodium arises from acrylate ligand adsorbed on the gold nanoparticle surface.[16] The mass of the beads decreased by 61 % during calcination, and the calcined beads had an average diameter of 0.80 mm as compared to a diameter of 1.90 mm for the original composite beads. The calcined products had a golden luster, as shown in Figure 2.

Electron micrographs of gold beads prepared under similar conditions are shown in Figure 3 (average bead diameter = 0.7 mm). Despite the high mass loss during calcination (60 % for this material), it was found that the beads retained the highly interconnected, "emulsion-templated" pore structure that was observed in the composite before calcination. Indeed, composite beads with lower gold loadings showed mass losses of up to 92 % after calcination while completely retaining both the bead morphology and the emulsion-templated porosity. Figures 3b–d show that the pores are highly interconnected and open to the bead surface. The standard method for measuring macropore size distributions is mercury intrusion porosimetry,[1,15,22] but this was not possible for these materials because of the formation of mercury–gold amalgams. As such, the average pore diameter for the material was estimated from scanning electron microscopy (SEM; >100 pores measured) to be 4.12 µm. This is similar to the pore size

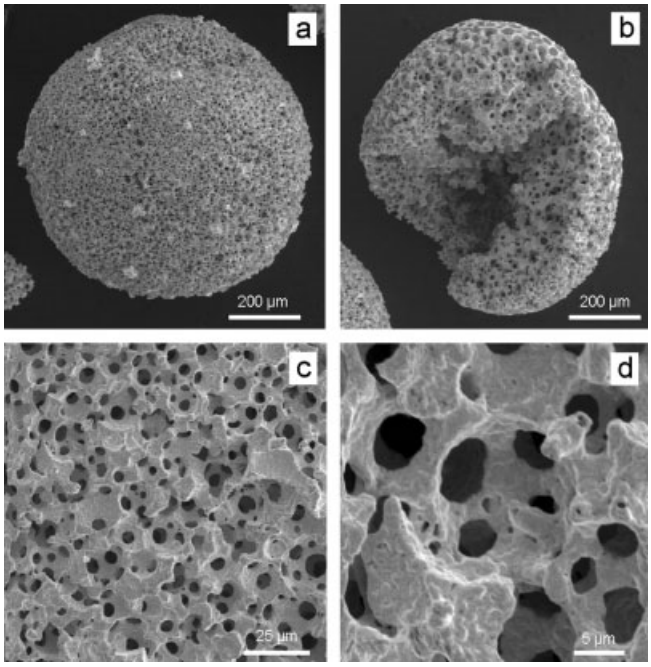

Figure 3. Electron micrographs of emulsion-templated gold beads prepared using gold nanoparticles as building blocks. a) Single emulsion-templated gold bead. b) Single cross-sectioned gold bead showing internal pore structure. c,d) Emulsion-templated pore structure on bead surface.

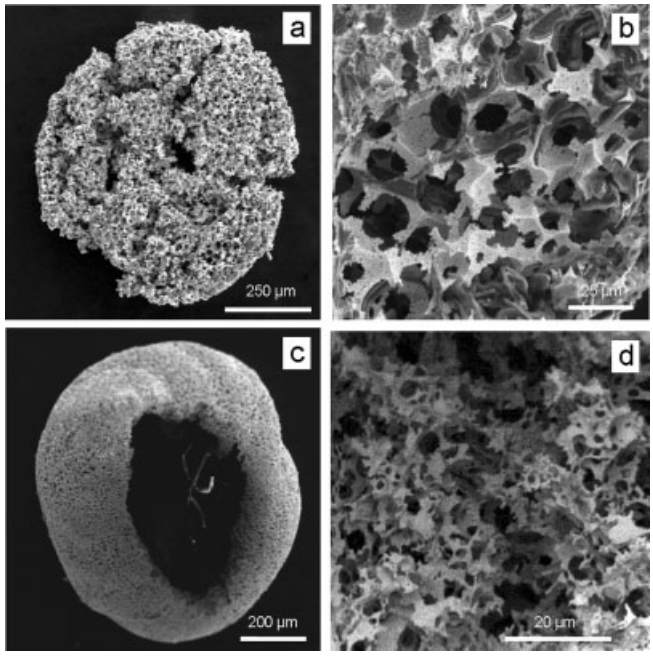

Figure 4. a) Electron micrograph of single cross-sectioned emulsion-templated gold bead prepared by in-situ reduction of $HAuCl_4$ followed by calcination. b) Electron micrograph showing the internal pore structure of the bead shown in (a). c) Electron micrograph of a hollow emulsion-templated gold bead prepared from polymer–gold composites with a non-uniform gold distribution (see, e.g., Fig. 1b). d) Internal surface of the emulsion-templated gold 'shell' of the hollow bead shown in (c).

measured by mercury intrusion porosimetry (4.85 μm) for emulsion-templated silica beads formed by a sol–gel polymerization route.[15] The bulk density of the gold beads was calculated (see Experimental) to be approximately 1.19 $g\,cm^{-3}$, which equates to a porosity of 93.83 % and a calculated pore volume of approximately 0.79 cm^3g^{-1}.

We believe that the gold nanoparticles are fused together to form bulk gold during calcination at 520 °C, which is consistent with the low surface area for the sample shown in Figure 3 ($< 5\ m^2g^{-1}$) as measured by gas sorption. The average pore diameter in these beads (~ 4 μm) is much larger than that observed in gold microspheres prepared from commercially available macroporous resins;[14] indeed, the average pore size in our structures is approximately equal to the radius of the beads formed by that route.

As a comparison, we also prepared porous gold beads using a second method. Emulsion-templated PAM beads were soaked in an aqueous solution of $HAuCl_4$, washed, and then filtered to yield a yellow $HAuCl_4$–PAM composite. The gold salt was then reduced in situ using a fresh solution of $NaBH_4$ in water, which gave rise to dark brown beads (33 wt.-% mass increase). The composite products were calcined as before to yield porous gold beads. Figures 4a,b show the pore structure of the calcined gold beads prepared via this "gold salt" route. The walls of the material contained additional porosity that was not present in the materials prepared using gold nanoparticles (see comparison of Figs. 3d and 4b). One interpretation for this difference is that the gold salt infuses into the interior of the water-swollen PAM matrix, while the gold nanoparticles are largely deposited on the PAM surface: as such, the swollen hydrogel structure is templated during reduction of the gold salt, which gives rise to the additional porosity observed in Figure 4b. It is also possible that this difference stems from the fact that the gold loading for the composite formed using the gold salt was lower than that observed for the material derived from the metal nanoparticles.

Since it is possible to control the distribution of the metal nanoparticles throughout the PAM–gold composite materials (see Figs. 1b,c and discussion above), we were also able to generate porous gold beads with more complex structures.[23] Figure 4c shows a fractured gold bead that was formed by calcining a composite with a non-uniform distribution of nanoparticles, similar to that shown in Figure 1b. The "shell" of the gold bead (thickness approximately 100 μm) has an emulsion-templated structure, as observed previously, but the core of the bead is hollow because the gold particles did not penetrate into the centre of the PAM scaffold. Figure 4d shows the pore structure at higher magnification; this image was recorded in the interior of the bead (i.e., the inner surface of the emulsion-templated gold shell). We believe that complex structures of this type with large, emulsion-templated pores could find a number of uses; for example, the porous gold shell should be selectively permeable to particles or biological species of diameters less than about 5 μm.

ADVANCED MATERIALS

While our initial studies have focused on porous gold, we believe that this method is relatively generic and could be applied to other nanoparticulate building blocks (e.g., other metals, metal oxides, inorganics). As an example, we have formed porous emulsion-templated silica beads by immersing PAM bead scaffolds in a colloidal solution of LUDOX HS-30 silica (average diameter = 20–40 nm). As in the case of gold nanoparticles, the colloidal silica was deposited on the PAM surface. Calcination lead to silica beads with emulsion-templated macropore structures that were similar to those formed using gold. The PAM–silica composite beads had a surface area of 69.5 $m^2 g^{-1}$ and a macropore volume (measured by mercury intrusion porosimetry) of 1.10 $cm^3 g^{-1}$. After calcination, the surface area increased to 160.6 $m^2 g^{-1}$ and the macropore volume increased to 1.90 $cm^3 g^{-1}$. Templated silica beads of this type could be useful, for example, as catalyst supports, but the mechanical strength of the structures was relatively low. This problem was solved by sintering the materials at 1450 °C. The sintered beads could withstand prolonged stirring in solvents without fracturing, although sintering also caused a reduction in the surface area and the pore volume of the materials.

In summary, we have developed a two-step method for producing emulsion-templated gold beads (0.5–1 mm diameter) with large pore volumes and average macropore diameters of around 4 μm. It would be relatively simple to produce bulk quantities of material since the polymer scaffold beads can be prepared semi-continuously on a kilogram scale. It should also be possible to reduce or even eliminate organic solvent usage by using supercritical fluids in the production stage.[24] When gold nanoparticles are used as building blocks, we observe complete replication of the original polymer macrostructure. It is possible to control the distribution of gold particles throughout the porous polymer beads. This allows us to generate quite complex structures such as hollow gold beads with a porous, emulsion-templated shell. This method is versatile, and it should be possible to generate a wide range of porous inorganic materials (e.g., silica) starting from a single batch of templated polymer beads. This deposition method using nanoparticulate building blocks has very significant advantages over the sol–gel emulsion templating approach that we described previously.[15] In particular, one can synthesize a large batch of polymer beads that will serve as a template for a wide range of materials, and it is not necessary to carry out time-consuming reoptimization of the emulsion stability for each new system that is studied.

Experimental

Emulsion-templated PAM beads were prepared by O/W/O sedimentation polymerization, as described previously [1]. The PAM beads were then soaked in aqueous gold nanoparticle solutions [16] for 1–2 weeks. Alternatively, the polymer beads were soaked in aqueous $HAuCl_4$ solution (20 mM) for 1 week and the gold salt was then reduced in situ. The wet composite beads were filtered and placed in an excess of isopropanol for at least 4 h. After filtering and drying under vacuum at room temperature, the composite beads were calcined using a similar procedure to that described elsewhere [15]. Bead morphologies were investigated with a Hitachi S-2460 N scanning electron microscope. Gold beads and gold composite beads were mounted on aluminum studs using adhesive graphite tape without sputter coating. Bead surface areas were measured by the Brunauer–Emmett–Teller (BET) method using a Micromeritics ASAP 2010 nitrogen sorption analyzer. Samples were outgassed for 15 h at 150 °C under vacuum before analysis. Bulk densities and pore volumes for the porous gold beads were estimated by calculating the average bead volume (from SEM measurements) and from knowledge of the accurate sample mass and the absolute density of gold (19.3 $g\,cm^{-3}$).

Received: September 11, 2003

[1] H. Zhang, A. I. Cooper, *Chem. Mater.* **2002**, *14*, 4017.
[2] N. R. Cameron, D. C. Sherrington, *Adv. Polym. Sci.* **1996**, *126*, 163.
[3] X. He, D. Antonelli, *Angew. Chem. Int. Ed.* **2002**, *41*, 214.
[4] D. van Noort, D.-F. Mandenius, *Biosens. Bioelectron.* **2000**, *15*, 203.
[5] D. van Noort, D.-F. Mandenius, *Mikrochim. Acta* **2001**, *136*, 49.
[6] C. Ji, P. C. Searson, *J. Phys. Chem. B* **2003**, *107*, 4494.
[7] Y. Ding, J. Erlebacher, *J. Am. Chem. Soc.* **2003**, *125*, 7772.
[8] J. Erlebacher, M. J. Aziz, A. Karma, N. Dimitrov, K. Sieradzki, *Nature* **2001**, *410*, 450.
[9] O. D. Velev, P. M. Tessier, A. M. Lenhoff, E. W. Kaler, *Nature* **1999**, *401*, 548.
[10] P. N. Bartlett, J. J. Baumberg, P. R. Birkin, M. A. Ghanem, M. C. Netti, *Chem. Mater.* **2002**, *14*, 2199.
[11] F. C. Meldrum, R. Seshadri, *Chem. Commun.* **2000**, 29.
[12] D. Walsh, L. Arcelli, T. Ikoma, J. Tanaka, S. Mann, *Nat. Mater.* **2003**, *2*, 386.
[13] A. Kulak, S. A. Davis, E. Dujardin, S. Mann, *Chem. Mater.* **2003**, *15*, 528.
[14] D. G. Shchukin, R. A. Caruso, *Chem. Commun.* **2003**, 1478.
[15] H. Zhang, G. C. Hardy, M. J. Rosseinsky, A. I. Cooper, *Adv. Mater.* **2003**, *15*, 78.
[16] I. Hussain, M. Brust, A. J. Papworth, A. I. Cooper, *Langmuir* **2003**, *19*, 4831.
[17] A. Kumar, S. Mandal, P. R. Selvakannan, R. Pasricha, A. B. Mandale, M. Sastry, *Langmuir* **2003**, *19*, 6277.
[18] K. Mukhopadhyay, S. Phadtare, V. P. Vinod, A. Kumar, M. Rao, R. V. Chaudhari, M. Sastry, *Langmuir* **2003**, *19*, 3858.
[19] A. G. Kanaras, Z. X. Wang, A. D. Bates, R. Cosstick, M. Brust, *Angew. Chem. Int. Ed.* **2003**, *42*, 191.
[20] R. Elghanian, J. J. Storhoff, R. C. Mucic, R. L. Letsinger, C. A. Mirkin, *Science* **1997**, *277*, 1078.
[21] N. Husing, U. Schubert, *Angew. Chem. Int. Ed.* **1998**, *37*, 23.
[22] R. Butler, C. M. Davies, A. I. Cooper, *Adv. Mater.* **2001**, *13*, 1459.
[23] C. Graf, A. van Blaaderen, *Langmuir* **2002**, *18*, 524.
[24] H. Zhang, A. I. Cooper, *Macromolecules* **2003**, *36*, 5061.

